A Fault-Tolerant Approach to Helicopter Swashplate Control

Bruce K. Walker*
Massachusetts Institute of Technology, Cambridge, Massachusetts
and
Eliezer Gai† and Mukund N. Desai‡
Charles Stark Draper Laboratory, Inc., Cambridge, Massachusetts

A novel method for controlling the orientation of a helicopter swashplate is developed from basic principles and evaluated by simulation. The method applies to rise-and-fall swashplates which are controlled by redundant actuators for the purpose of achieving survivability and fault-tolerance. The suggested control scheme maintains all of the actuators in an active state, thereby avoiding transient effects following component failures and also making possible the use of simple but effective comparison-type failure diagnostics. In addition, the scheme alleviates the "force-fighting" which is prevalent in redundant actuation designs via a minimum norm concept which conserves hydraulic energy. A simulation of the swashplate dynamics is then developed and used to evaluate the performance of the new controller design relative to that of other suggested multiactuator swashplate controller designs in terms of dynamic response, alleviation of force fights, and detection of actuator failures.

Introduction

THE control of the attitude and flight direction of helicopters and other airborne rotor craft is effected primarily by commanding the tilt of the lift vector provided by the main rotor. The magnitude and orientation of the lift vector for constant rotor speeds is determined by the aerodynamic lift force provided by each rotor blade, which in turn is determined by the pitch angle of the blade. The blade pitch at a given angular position around the main rotor swashplate (assuming a so-called "rise and fall" swashplate) is controlled by the position at that point of the swashplate. Thus, the orientation of the plane defined by the swashplate (which is assumed to be rigid) is the primary factor in determining the dynamical behavior of the aircraft. Control of swashplate orientation is generally provided by two-stage hydraulically powered actuators mounted on the swashplate periphery. These actuators must maintain the orientation of the swashplate despite disturbing forces resulting from nonsteady aerodynamic forces on the blades and inertial and gravitational effects.

Since the control of the swashplate orientation is crucial to the flight safety of the vehicle and to its flight performance capability, the reliability and survivability of the swashplate control system has recently become an issue. The goal of a fault-tolerant swashplate controller is to provide complete control of the swashplate orientation despite the loss of one or more actuators due to component failure, damage, or false indications of failure resulting in actuator shutdown. This requires the use of redundant actuators on the swashplate and of some automated means of detecting and identifying actuator malfunctions and removing the offending actuator from operation. In addition, the control strategy for the actuators must reflect the presence of more actuators than are necessary for swashplate control.

Submitted April 4, 1983; revision received March 23, 1984.

*Assistant Professor, Department of Aeronautics and Astronautics. Member AIAA.
†Section Chief, Integrated Systems Division. Member AIAA.
‡Technical Staff, Integrated Systems Division. Member AIAA.

Several options exist for the configuration of fault-tolerant swashplate control schemes. Since the task of the control strategy is to properly orient the swashplate plane, a minimum of three operational noncollinear actuators is required at all times. One possible controller design, based on standard redundant actuation practice, involves the use of multiple hydraulic rams in a force-summing configuration mounted at each of three noncollinear points around the swashplate periphery. Although this strategy provides the redundancy necessary to survive component failures, it is highly vulnerable to structural damage. Its viability is increased if the three mounting points and the nearby hardware can be armored, but added armor implies additional weight and is therefore an unattractive option. Also, the force-summing configuration requires the use of at least two actuators at each mounting point to tolerate a single failure for a minimum total of six. To achieve a high level of actuator fault detectability and to tolerate multiple failures, at least three actuators are desirable at each mounting point implying a total of at least nine. The alternative swashplate actuation strategies to be discussed presently will, in general, achieve similar levels of reliability using fewer actuators.

More recently, actuation configurations involving more than three mounting points have been suggested.[1,2] A drawback exists, however, when the actuators are independently controlled, as they frequently are, to achieve specified local positions dictated by the desired swashplate orientation. If all of the redundant actuators are simultaneously active, a condition known as a "force-fight" can develop. This occurs when due to measurement biases, hardware misalignments, or other sources, one (or more) of the sensed actuator mount positions deviates from its desired value while the remaining indicated positions do not, thereby causing one actuator to begin needlessly correcting its perceived position error while the others exert effort to maintain the status quo. One way to avoid a force-fight is to disable all but three noncollinear actuators, designated the "primary" actuators, and use one or more of the disabled "secondary" actuators only as replacements in response to indicated malfunctions of the three primary actuators. This simple "bypass" approach is fraught with disadvantages, including possible startup transients for the secondary actuators when

they are needed, asymmetric actuation geometry, and preclusion of the use of comparison failure detection tests for detecting and identifying actuator malfunctions which tend to be more reliable than built-in hardware tests.

Another force-fight alleviation scheme involves the designation of three primary actuators and the addition of pressure sensors and independent pressure control loops to the secondary actuators.[1,2] All of the nonfailed actuators are kept active at all times, but the secondary actuators are commanded through low-pass compensators to achieve zero differential pressure across their driving rams. This has the effect of disabling the secondary actuators in the steady state while allowing them to aid the primary actuators in responding to sudden changes in the desired swashplate position and also keeping them active so as to avoid startup transients should a primary actuator malfunction. This "pressure null" strategy still suffers from the disadvantages of asymmetric geometry and reliance on built-in testing which were discussed above for the bypass approach.

In this paper, a strategy is suggested for fault-tolerant swashplate control which avoids these difficulties while still alleviating force fights. This strategy is then tested on a complete simulation of the dynamics of a swashplate and its associated hardware. The next section describes the control strategy, derives its theoretical basis, discusses some issues related to redundancy management, and points out some properties of the controller which have a bearing on its implementation. The theory behind the swashplate dynamics simulation is briefly summarized next, and the results of the simulation are then presented for several representative scenarios using the suggested swashplate control scheme and others. Conclusions and a summary of our ongoing efforts in this area conclude the paper.

Minimum Norm Fault-Tolerant Swashplate Controller

In this section, a novel concept is described for controlling the orientation of the swashplate using five or more spatially distributed actuators mounted on the swashplate periphery. This controller design concept maintains the quasi-independence of the feedback loops governing the behavior of each actuator; however, it possesses some advantages relative to the designs described in the preceding section. The advantages include the following. 1) The tendency of the actuators to force-fight is reduced because the control strategy is designed to minimize the total hydraulic energy expended in controlling the swashplate. 2) Standard comparison tests can be employed for fault detection and isolation (FDI). This control concept, herein referred to as the "minimum norm" strategy, is currently pending for a U.S. patent.

Underlying Philosophy

Assume that the tipping of the swashplate is limited to small angles and that the swashplate is rigid. Therefore, the actuators provide forces which are always normal to the nominal swashplate plane. Consider N peripherally mounted actuators on the swashplate with $N>3$ and with a mounting radius of R. The case of $N=5$ is illustrated in Fig. 1 for a symmetric mounting pattern. This symmetry is not necessary for the development; however, asymmetric actuator patterns are generally undesirable for reasons related to load ratings. Figure 1 also illustrates the convention for defining the geometry of the swashplate actuators, to each actuator there corresponds an ordered pair (x_i, y_i) describing its mounting position on the swashplate periphery.

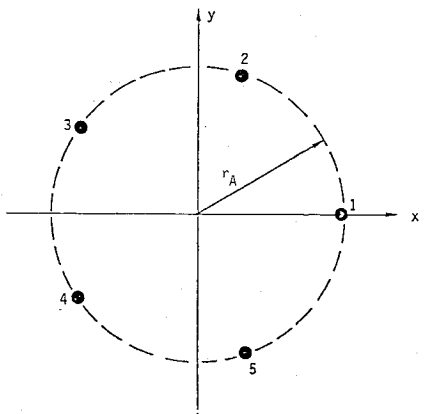

Fig. 1 Actuator configuration ($N=5$).

Let f_i be the upward vertical force applied to the swashplate by the ith actuator. Then the total vertical force applied to the swashplate is given by

$$F=\sum_{i=1}^{N} f_i \tag{1}$$

The rolling and pitching torques applied to the swashplate are given by

$$T_\phi=\sum_{i=1}^{N} f_i \cdot Ry_i \tag{2}$$

$$T_\theta=\sum_{i=1}^{N} f_i \cdot (-Rx_i) \tag{3}$$

In vector-matrix form, Eqs. (1-3) become:

$$\begin{bmatrix} F \\ T_\phi \\ T_\theta \end{bmatrix} = \begin{bmatrix} 1 & 1 & \dots & 1 \\ R_y 1 & Ry_2 & \dots & Ry_N \\ -Rx_1 & -Rx_2 & \dots & -Rx_N \end{bmatrix} f \tag{4}$$

Using the normalized torques $\tau_\phi \triangleq T_\phi/R$ and $\tau_\theta = T_\theta/R$, Eq. (4) becomes

$$\begin{bmatrix} F \\ \tau_\phi \\ \tau_\theta \end{bmatrix} = Cf \tag{5}$$

where f is the N-vector of actuator forces and C is a constant matrix defined entirely by the geometry:

$$C=\begin{bmatrix} 1 & 1 & \dots & 1 \\ y_1 & y_2 & \dots & y_N \\ -x_1 & -x_2 & \dots & -x_N \end{bmatrix} \tag{6}$$

For a set of N actuators with identical characteristics, the force provided by the ith actuator is related to the differential pressure Δp_i across the ram piston of the actuator by

$$f_i = A_R \Delta p_i \tag{7}$$

where A_R is the ram piston area. It is assumed here that the actuators are balanced, i.e., that they present the same ram piston surface area to each side of the ram cylinder. Substituting Eq. (7) into Eq. (5) yields:

$$\begin{bmatrix} F \\ \tau_\phi \\ \tau_\theta \end{bmatrix} = CA_R \Delta p \tag{8}$$

where Δp is the N-vector of actuator ram differential pressures.

If measurements of the differential pressures are available, then Eq. (8) provides a means for calculating the resultant

vector of force and torques applied to the swashplate by the actuators. Note, however, that for $N>3$ there exist $N-3$ degrees of freedom because Eq. (3) represents three linear equations in N unknowns. Using those additional degrees of freedom, one can find the vector Δp^* of differential pressures which are such that the force and torques applied to the swashplate are identical to those which are calculated using the measured Δp in Eq. (8) but for which the quantity:

$$J=\sum_{i=1}^{N}(\Delta p_i^*)^2=(\Delta p^*)^T\Delta p^* \tag{9}$$

is minimized. The quantity J in Eq. (9) is directly proportional to the hydraulic energy which is expended in providing the actuator forces f. Therefore, minimization of J is equivalent to the minimization of expended hydraulic energy. Note also that J is the Euclidean norm of Δp^*, hence Δp^* has "minimum norm," a circumstance which lends the control strategy its name.

The solution Δp^* can easily be derived by using the Lagrange multiplier method[3,4] to adjoin the constraint of Eq. (8) to Eq. (9). The solution is

$$\Delta p^*=C^T[CC^T]^{-1}C\Delta p \tag{10}$$

where Δp is again the N-vector of measured ram differential pressures. The control strategy then consists of a primary loop for each actuator, which controls the position of the actuator such that the desired swashplate orientation is achieved, surrounded by an outer loop, which usually includes a low-pass compensator similar to Refs. 1 and 2, to drive Δp to Δp^* in the steady state. This controller structure is illustrated by the block diagram of Fig. 2. Thus, swashplate position control is maintained, the control loops for each actuator remain essentially independent, all of the actuators remain active, and the energy expended under steady-state conditions is minimized if the minimum norm strategy is employed.

Fault Detection and Isolation

The primary motivation for including redundant actuators in the design of a swashplate controller is to enhance the reliability and survivability of the system. This implies that some type of automated fault detection and isolation (FDI) scheme is to be included in the controller software. In the Introduction it was pointed out that some of the suggested methods for controlling the swashplate actuators have the effect of forcing the FDI strategy to be dependent solely on built-in tests (BITs) for its information. The minimum norm control strategy, however, allows the designer to utilize comparison-type tests for FDI. The latter tend to be more reliable in terms of failure coverage than BITs. In the succeeding paragraphs, the implementation and advantages of comparison tests for FDI in conjunction with the minimum norm control strategy are described.

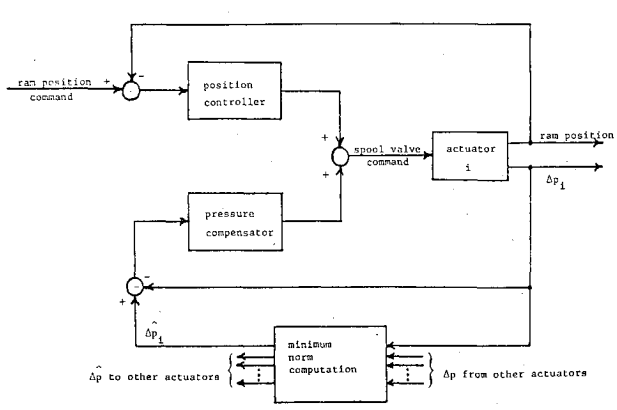

Fig. 2 Minimum Norm Controller block diagram.

Consider the quantities Δp_r given by the vector difference

$$\Delta p_r \triangleq \Delta p-\Delta p^* \tag{11}$$

henceforth referred to as the *pressure residuals*. In the steady state, the minimum norm control strategy tends to drive the pressure residuals to zero. However, the pressure residuals will deviate from zero upon the sudden onset of one of several types of actuator failures. Examples of such failure types and their effect on the pressure residuals include 1) loss of pressure on one side of ith piston – large Δp_i and corresponding $(\Delta p_r)_i$, 2) One side of ith piston open to source (or drain), same effect as (1), 3) Ram piston i jammed, eventual buildup of Δp_i as position loop commands a change of position with same effects as (1) and (2), and 4) offset (or jam) of ith control valve, bias in Δp_i which, if sufficiently large, appears as a bias in $(\Delta p_r)_i$.

The manifestation of these and other actuator failures as sudden biases in the corresponding component of the pressure residual vector suggests the following FDI strategy.

Declare that no failure is present if

$$(\Delta p_r)_i<T_p \quad \text{for} \quad i=1,\ldots,N \tag{12}$$

Otherwise, isolate instrument i as failed where:

$$i=\arg\max_{j=1,\ldots,N}|(\Delta p_r)_j| \tag{13}$$

Ther are several limitations to this strategy. One is induced by the dynamics of the load transmitted to the swashplate by the rotor blade pitch links. Since the minimum norm control strategy drives the pressure residuals to zero only in the steady state, any load dynamics which occur at frequencies higher than that to which the pressure control loop can respond will produce nonzero pressure residuals and, therefore, may cause false alarms by the FDI aside from those attributable to observation noise. Also, it is necessary that N be at least as great as five in order for the FDI strategy to be capable of isolating the failure to a particular actuator. It can easily be shown that Δp_r always lies in a space of dimension N-3. For $N=3$, this implies that no pressure residuals exist, a fact which could also be deduced from the fact that Eq. (8) has the unique solution Δp when $N=3$ because C is then invertible.

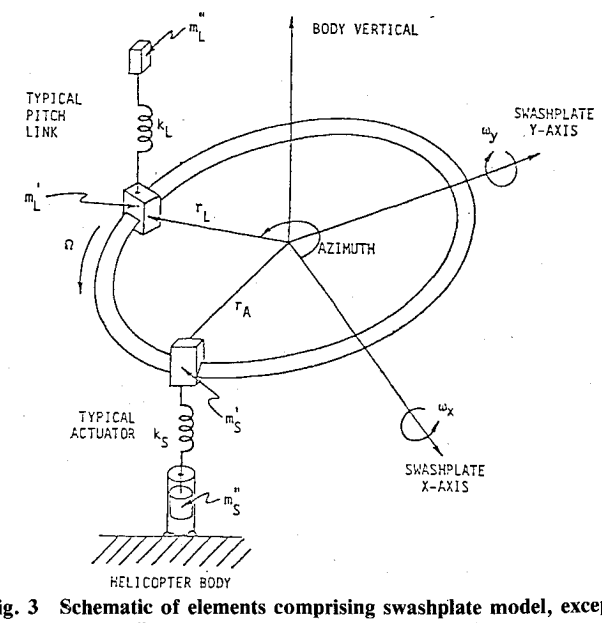

Fig. 3 Schematic of elements comprising swashplate model, except for actuator detail.

For $N=4$, this result implies that the pressure residuals have a specific relationship to one another at all times and that only the magnitude and polarity of this relationship can vary. As a result, when $N=4$ the pressure residuals can be used only to detect the presence of a failure while isolation must rely on BITs. For $N\geq 5$, the parity space in which Δp_r lies is at least a plane, and directions in this space can be defined corresponding to failures in each of the actuators with which the direction of Δp_r can be compared. For further discussion of parity spaces and their relationship to FDI procedures, see Ref. 5.

The FDI software necessary for detecting and identifying sensor faults can be designed separately if sufficient sensors are present to accommodate algorithmic FDI tests. It is worthy of note, however, that certain sudden sensor failures of the bias type are also manifest as changes in Δp_r. These include bias failures of the Δp transducers, of the ram piston position transducers (LVDT's), and of the control valve position transducers. This means that while separate redundancy management strategies are desirable for the sensors, the pressure residuals can be used to deect and isolate an actuator which is affected by a sensor failure.

Implementation Considerations

One goal in the design of many recently proposed systems is the decentralization of the computational burden inherent to its implementation. The minimum norm control strategy and the associated FDI architecture are well-suited to this goal. To implement the control strategy, a localized processor dedicated to a particular actuator need only have available as data the local values of ram piston position and ram differential pressure (available as local measurements), the commanded ram piston position (available from the flight control computer either directly or via computation from the known geometry of the actuator and the commanded vertical position, pitch, and roll of the swashplate), and the differential pressures of the remaining actuators. In read-only memory, the local processor need have only the appropriate row of coefficients of the matrix $[I_N - C^T(CC^T)^{-1}C]$ and any compensation coefficients (and geometry coefficients if the actuator ram position is not available directly from flight control). From this information, the local processor can compute the servovalve input and form the local pressure residual, the latter of which can be transmitted to the processor which performs the FDI algorithm. Note that, neglecting any compensation dynamics other than a scaling and assuming commanded ram piston position is available directly, only $N+1$ multiply operations, $N+2$ add operations, and one sign change are necessary to produce the local servovalve input and pressure residual.

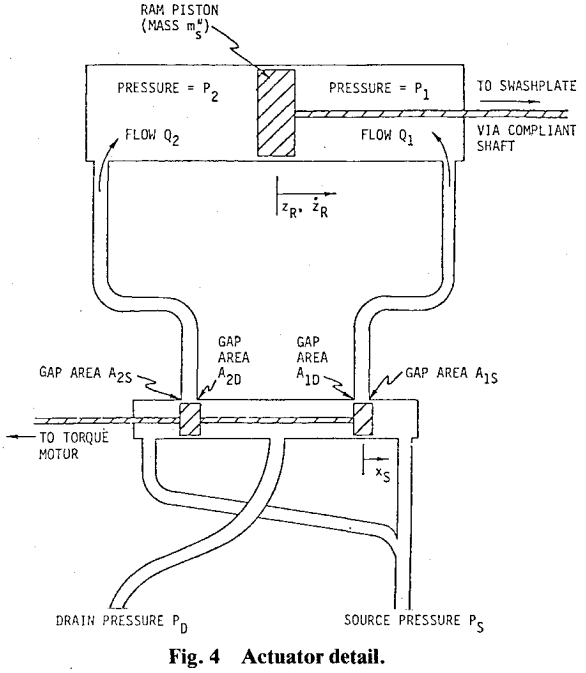

Fig. 4 Actuator detail.

Simulation Development

In order to investigate the performance of the minimum norm swashplate controller and the associated FDI strategy based on the pressure residuals, a simulation of the dynamics of a swashplate driven by multiple actuators must be developed. The mathematical model of the swashplate and actuator dynamics is developed in Ref. 7 and, briefly, in the Appendix. It is summarized below. The section immediately thereafter briefly discusses some simplifications for the implementation of the simulation.

Summary of Basic Model

The dynamical system of interest is comprised of the following elements (see Figs. 3 and 4):

1) A rigid swashplate which has only three degrees of freedom of motion with respect to the helicopter: vertical translation (or collective), pitch rotation, and roll rotation.

2) Exactly N compliant actuator shafts joining the swashplate to the actuator ram pistons, mounted circularly about the main rotor hub.

3) Exactly N_L compliant pitch links joining the swashplate to the blade pitch arms, also mounted circularly and rotating.

4) Hydraulic actuators (N of them) driven by standard servovalves (Fig 4). The servovalve dynamics are first-order.

In addition to the above, the following three assumptions are made in the modeling:

1) The actuator shafts are of sufficient length and the swashplate tipping is limited to angular magnitudes sufficiently small so that essentially 100% of the actuator force is applied parallel to the fixed vertical axis of the helicopter body. Any force which is not directed in this fashion would merely be absorbed by the swashplate mounting and, hence, would not contribute to swashplate motion.

2) The pitch link loads applied by the blades are known as functions of time or of the spatial blade location.

3) The body motion quantities of angular rate, angular acceleration, and the nongravitational acceleration component along body-vertical are known for a body-fixed point located a distance Z_0 directly beneath the equilibrium position of the swashplate center along the body vertical. The body-vertical component of gravitational acceleration also is known.

A brief summary of the derivation appears in the Appendix. With the nomenclature of Table 1, the resulting dynamical equations to be solved are:

$$\ddot{Z}_s = -a^{(B)}{}_z + g^{(B)}{}_z + \left[\omega_B^{(B)2}{}_x + \omega_B^{(B)2}{}_y\right] Z_0 + Z_x + \frac{1}{M_s'}\sum_{i=1}^{N} f_{Ai} - \frac{1}{M_s'}\sum_{j=1}^{N_L} f_{Lj} \tag{14}$$

$$\dot{\omega}_x = \frac{I_y T_X - I_{xy} T_Y}{I_x I_y - I_{xy}^2} \tag{15}$$

$$\dot{\omega}_y = \frac{I_x T_Y - I_{xy} T_X}{I_x I_y - I_{xy}^2} \tag{16}$$

$$\dot{q} = \tfrac{1}{2}\begin{bmatrix} 0 & -\omega_x & -\omega_y & 0 \\ \omega_x & 0 & 0 & -\omega_y \\ \omega_y & 0 & 0 & \omega_x \\ 0 & \omega_y & -\omega_x & 0 \end{bmatrix} q \tag{17}$$

Table 1 Nomenclature for simulation model

Symbol	Represents	Constant or time-variant	Function of
$(a^{(B)})_z$	Body vertical component of helicopter's nongravitational acceleration	TV	–
A_R	Ram piston effective area	C	–
A_{1D}, A_{2D}	Orifice area exposing each side of hydraulic cylinder to drain pressure	TV	x_s
A_{1S}, A_{2S}	Orifice area exposing each side of hydraulic cylinder to source pressure	TV	x_s
C_w	Orifice flow coefficient	C	–
f_{A_i}	Force applied by actuator shaft i to swashplate	TV	Δs_i
f_{L_j}	Force applied by pitch link shaft j to swashplate	TV	$\Delta \ell_j$
F_{A_i}	Force applied to actuator shaft i by actuator i	TV	ΔP_i
F_{L_j}	Force applied to pitch link shaft j by blade j	TV	–
$(g^{(B)})_z$	Body vertical component of gravitational acceleration	TV	–
I_i	Current command into servovalve for actuator i	TV	Command
I_r	Swashplate mass moment of inertia about rotor axis	C	–
I_t	Swashplate mass moment of inertia about transverse axis.	C	–
I_x, I_y, I_{xy}	Mass moments of inertia of swashplate assembly (including pitch link masses and actuator shaft masses) about respective swashplate-fixed axes	TV	I_t, θ_j, actuator geometry
k_I	Servovalue current-to-position gain	C	–
k_L	Pitch link shaft equivalent spring constant	C	–
k_s	Actuator shaft equivalent spring constant	C	–
$\Delta \ell_j$	Deviation from nominal of pitch link length (positive = extended)	TV	[a]
m_L'	Pitch link mass at swashplate end	C	–
m_L''	Pitch link mass at blade end	C	–
m_s'	Actuator shaft mass at swashplate end	C	–
m_s''	Actuator shaft mass at piston end	C	–
M_s	Swashplate mass	C	–
M_s'	$\triangleq M_s + \sum_{i=1}^{N} m_s' + \sum_{j=1}^{N_L} m_L'$	C	See formula
P_D	Drain pressure	C	–
P_S	Source pressure	C	–
P_1, P_2	Actuator cylinder chamber pressure, nearest and furthest from swashplate, respectively	TV	[a]
ΔP	Differential pressure, $= P_2 - P_1$	TV	See formula
q	Quaternion representing swashplate attitude with respect to its equilibrium position normal to main rotor axis	TV	[a]
Q_1, Q_2	Net flows into actuator cylinder, nearest and furthest from swashplate, respectively	TV	See Appendix
r_A	Radius of circular actuator mounting pattern	C	–
r_L	Radius of circular pitch link mounting pattern	C	–
Δs_i	Deviation from nominal of actuator shaft length (positive = extended)	TV	[a]
t_1^T, t_2^T, t_3^T	Rows of transformation matrix from body-fixed axes to swashplate axes	TV	q
t_{ij}	Element (i,j) of body axes to swashplate axes transformation matrix	TV	q
T_x, T_y	Torque applied to swashplate about, respectively, roll and pitch axes due to shaft forces, Coriolis effects, centripetal effects, inertia dynamics, etc.	TV	Many variables
V_{total}	Total fluid volume of an actuator	C	–
ΔV	Change in fluid volume on either side of actuator cylinder due to deviation of piston from nominal position	TV	See Appendix
x_{s_i}	Servovalue deviation from nominal for actuator i	TV	[a]
$\ddot{z}_{Lj}$	Acceleration (inertially referred) of swashplate end of pitch link, positive upward	TV	$a^{(B)}$, body rates, $Z_s, \omega_x, \omega_y, \Omega$, geometry
$\dot{z}_{R_i}$	Velocity (referred to helicopter) of ram piston of actuator i, positive upward	TV	See Appendix
$\ddot{z}_{Si}$	Acceleration (inertially referred) of swashplate end of actuator shaft, positive upward	TV	$a^{(B)}$, body rates, Z_s, ω_x, ω_y
Z_S	Deviation from nominal along body vertical of swashplate position (i.e., collective displacement)	TV	[a]
Z_0	Nominal distance (vertical) from helicopter, c.g. to undisplaced swashplate center	C	–
β	Bulk modulus of hydraulic fluid	C	–
θ_j	Angular position of pitch link j with respect to x-axis of swashplate frame	TV	Ω
τ_s	Servovalve dynamics time constant	C	–
$\omega_B^{(B)}$	Inertially referred angular velocity vector of helicopter coordinatized in body axes	TV	–
ω_x, ω_y	Angular velocities of swashplate with respect to helicopter (roll rate, pitch rate)	TV	[a]
Ω	Rotor angular velocity	C	–

[a] Dynamical state variables.

$$\ddot{\Delta}s_i = -\left(g^{(B)}\right)_z + \ddot{z}_{Si} + \left[\left(\omega_{IB}^{(B)}\right)_x^2 + \left(\omega_{IB}^{(B)}\right)_y^2\right](S+\Delta s_i)$$

$$-\frac{k_s}{m_s''}\Delta s_i - \frac{1}{m_s''}F_{Ai} \qquad i=1,\ldots,N \qquad (18)$$

$$\ddot{\Delta}l_j = \left(g^{(B)}\right)_z - \ddot{z}_{Lj} + \left[\left(\omega_{IB}^{(B)}\right)_x^2 + \left(\omega_{IB}^{(B)}\right)_y^2\right](L+\Delta l_j)$$

$$-\frac{k_L}{m_L''}\Delta l_j - \frac{1}{m_L''}F_{Lj} \qquad j=1,\ldots,N_L \qquad (19)$$

$$\dot{P}_1 = \frac{\beta(Q_1 + A_R\dot{z}_{Ri})}{\frac{1}{2}V_{\text{total}} - \Delta V} \qquad i=1,\ldots,N \qquad (20a)$$

$$\dot{P}_2 = \frac{\beta(Q_2 - A_R\dot{z}_{Ri})}{\frac{1}{2}V_{\text{total}} - \Delta V} \qquad i=1,\ldots,N \qquad (20b)$$

$$\dot{x}_{S_i} = -\frac{1}{\tau_s}x_{S_i} + k_I I_i \qquad i=1,\ldots,N \qquad (21)$$

In terms of a state space representation of the system, the model will have $(N+2N_L+8)$ state variables. For example, for a five-actuator, four-blade system, there would be a total of 41 dynamical states.

Reduction of Model Complexity

For typical values of β and of the geometrical parameters of the actuator ram (V_{total} and A_R), Eqs. (20) can represent very stiff dynamics. Assuming $\Delta V \ll V_{\text{total}}$ and using Eq. (20), one obtains

$$\Delta\dot{P} = \dot{P}_2 - \dot{P}_1 = \frac{2\beta}{V_{\text{total}}}\left[Q_2(x_s) - Q_1(x_s) - 2A_R\dot{z}_R\right] \qquad (22)$$

where ΔP is the differential pressure for the actuator and the subscript i has been dropped for simplicity. If m_R is the total mass of the ram piston/shaft assembly and F_s is the force transmitted by the shaft, then

$$m_R\ddot{z}_R = -F_s + A_R\Delta P \qquad (23)$$

which, upon differentiation and substitution for $\Delta\dot{P}$, becomes

$$m_R\dddot{z}_R + \frac{4\beta A_R^2}{V_{\text{total}}}\ddot{z}_R = -\dot{F}_s + \frac{2\beta A_R}{V_{\text{total}}}\left[Q_2(x_s) - Q_1(x_s)\right] \qquad (24)$$

The homogeneous part of this equation represents an undamped oscillatory mode with natural frequency

$$\omega_n = 2A_R\sqrt{\frac{\beta}{m_R V_{\text{total}}}} \qquad (25)$$

which can be very large compared to the other modes of the system.

These stiff dynamics can be considered a boundary layer perturbation to the remaining slower dynamics. In this singular perturbation approach, these perturbations are assumed essentially to have reached steady state within a time interval which is short relative to the time constants associated with the remaining dynamics. The dynamical equations for the perturbations then reduce to algebraic equations and the number of differential equations to be integrated in the simulation is reduced.

An alternative approach leading to the same result is to assume that $m_R = 0$. This assumption has a dual interpretation: Instantaneous steady state is assumed for the compressibility dynamics, and the actuator shaft dynamics are assumed negligible. The actuator shaft extension model then reduces to a linear spring with spring constant k_s. Furthermore, an elegant physical interpretation can be given to the assumption that $m_R = 0$ if the second-order differential equation (24) for $\dot{z}_R$ is written as follows after m_R is set to zero

$$\dot{F}_s = -\frac{4\beta A_R^2}{V_{\text{total}}}\left[\dot{z}_R - \frac{1}{2A_R}(Q_2 - Q_1)\right] \qquad (26)$$

Define a new state variable

$$z_{R_{\text{ref}}} = \frac{1}{2A_R}\left[Q_2(x_s) - Q_1(x_s)\right] \qquad (27)$$

Then

$$\dot{F}_s = -\frac{4\beta A_R^2}{V_{\text{total}}}\left(\dot{z}_R - \dot{z}_{R_{\text{ref}}}\right) \qquad (28)$$

The steady state for the compressibility is achieved when $\dot{P}_2 = \dot{P}_1 = 0$ which also implies that $Q_2 = -Q_1 = A_R\dot{z}_R$ which, via Eq. (27), leads to $\dot{F}_s = 0$. This latter implication implies that Eq. (28) can be integrated to yield $F_s = -4\beta A_R^2(z_R - z_{R_{\text{ref}}})/V_{\text{total}}$ where it is assumed that zero force is applied by the actuator to the swashplate when z_R and $z_{R_{\text{ref}}}$ agree. This implies that the actuator can be represented by a spring with spring constant $4\beta A_R^2/V_{\text{total}}$ acting on the displacement $z_R - z_{R_{\text{ref}}}$ where the "reference ram position" $z_{R_{\text{ref}}}$ is controlled by the spool valve position through the equation $\dot{z}_{R_{\text{ref}}} = -Q_1(x_s)/A_R$ where the substitution $Q_2 = -Q_1$ has been made, thereby assuming the steady state for the flow rates.

It remains now to solve for the steady-state flow Q_1. This is accomplished as follows. An expression has been found for the force transmitted by the actuator to the shaft F_s. Recall that $\Delta P = F_s/A_R$ and that $\Delta P = P_2 - P_1$. The steady-state flow condition yields $Q_2 = -Q_1$ which, when combined with Eq. (A5) and $\Delta P = P_2 - P_1$ yields

$$A_{1S}\sqrt{P_s - P_1} - A_{1D}\sqrt{P_1 - P_D} + A_{2S}\sqrt{P_s - P_1 - \Delta P} - A_{2D}\sqrt{P_1 - (P_D - \Delta P)} = 0 \qquad (29)$$

Since the areas and the source and drain pressures are known, and since ΔP is a function only of z_R and $z_{R_{\text{ref}}}$, both of which are now state variables (or can be found from state variables), Eq. (29) is a nonlinear algebraic equation which can be solved for P_1. The method used in the simulation is the standard Newton-Raphson algorithm.[6] Having obtained P_1, Q_1 is easily determined from Eq. (A5a).

To determine F_s, use the fact that $z_R = z_s - \Delta s$. Assuming that the actuator shaft can be represented by a spring with spring constant k_s, then $\Delta s = -F_s/k_s$ and this, with the definition of z_R, can be substituted into the definition of F_s above yielding

$$F_s = -\frac{-4\beta A_R^2 k_s(z_s - z_{R_{\text{ref}}})}{4A_R^2 + k_s V_{\text{total}}} \qquad (30)$$

This is the force that the actuator applies to the swashplate.

Similarly, the pitch link shafts can be modelled as simple linear springs with spring constant k_L. As a result, the full pitch link load is transmitted to the swashplate.

The result of all of these assumptions is to reduce drastically the number of state variables describing the system and, hence, the number of differential equations that must be integrated in the simulation. Removed are the state variables P_1, P_2, Δs, and $\dot{\Delta}s$ for each actuator and $\dot{\Delta}l$ and Δl for each pitch link. Added is the state variable $z_{R_{\text{ref}}}$ for each actuator. The end result is that there are a total of $(2N+8)$ states representing the dynamics. This is in contrast to the original

simulation for which $(5N+2N_L+8)$ states were necessary. The size of the reduction is considerable when one reconsiders the case of five actuators and four pitch links. The previous simulation produced a 41-state model, while the current model has only 19 states.

Simulation Results

In this section, the simulation of the swashplate dynamics discussed in the preceding section is used to evaluate three alternative control strategies. The assumed characteristics of the swashplate hardware are summarized in Table 2. These characteristics were not chosen to be representative of any particular helicopter.

In the simulation studies, the Minimum Norm approach is compared to other approaches. All three approaches involve a similar primary position feedback but utilize differing strategies with regard to the feedback of actuator drive piston differential pressures. In the Bypass (B) approach, all but three of the actuators (designated the *active* actuators) have their drive pistons bypassed so that the differential pressures for these inactive actuators are always null. Thus, the inactive actuators provide no force to drive the swashplate. In the Pressure Null closure (PN) approach,[1,2] three of the actuators operate purely on position feedback. The remaining actuators, in addition to the position feedback, operate on differential pressure feedback signals which, after compensation, tend to drive the differential pressures for these actuators toward null. The compensation is present in order to limit this nulling behavior to low frequencies so that the position feedback is dominant at high frequencies. The Minimum Norm (MN) approach was discussed previously in this paper. As in the simulation development section, it is assumed that the swashplate tipping is small enough so that the actuators can be assumed to provide forces that are always directed normal to the nominal swashplate plane.

All of the simulated results are for the case of $N=5$ with symmetrically placed actuators (the STAR configuration of Ref. 1, as seen in Fig. 1. For this configuration;

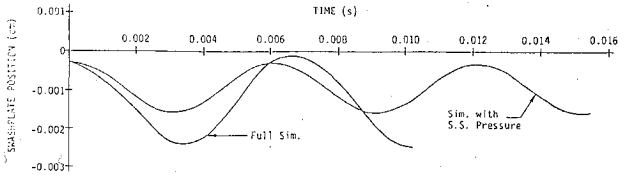

Fig. 5 Swashplate position as a function of time for the two simulations.

Table 2 Simulation parameters

Number of actuators, N	5 (evenly spaced round the periphery)
Number of pitch links, N_L	4 (also evenly spaced)
Swashplate diameter $2r_L$, $2r_A$	15 cm
Swashplate mass, M_S	30 kg
Nominal height above c.g., Z_0	180 cm
Actuator shaft length, S	21.6 cm
Actuator shaft mass, m_S'	7.9 kg
Actuator shaft spring constant, k_S	92.8×10^9 dyne/cm
Actuator ram area, A_R	19.4 cm^2
Actuator total volume, V_{total}	165 cc
Source pressure, P_S	3500 psi
Drain pressure P_D	500 psi
Fluid density, ρ	0.81 g/cm^3
Fluid bulk modulus, β	50×10^3 psi
Pitch link length, L	10 cm
Pitch link spring constant, k_L	92.8×10^9 dyne/cm
Pitch link mass, m_L'	10 kg
Rotor speed, Ω	180 rpm

$$C=\begin{bmatrix} 1 & 1 & 1 & 1 & 1 \\ 0 & R\cos 18^\circ & R\cos 54^\circ & -R\cos 54^\circ & -R\cos 18^\circ \\ -R & -R\sin 18^\circ & R\sin 54^\circ & R\sin 54^\circ & -R\sin 18^\circ \end{bmatrix} \tag{31}$$

so that the geometrical transformation of Eq. (10) becomes:

$$C^T[CC^T]^{-1}C = \begin{bmatrix} 0.6 & 0.324 & -0.124 & -0.124 & 0.324 \\ 0.324 & 0.6 & 0.324 & -0.124 & -0.124 \\ -0.124 & 0.324 & 0.6 & 0.324 & -0.124 \\ -0.124 & -0.124 & 0.324 & 0.6 & 0.324 \\ 0.324 & -0.124 & -0.124 & 0.324 & 0.6 \end{bmatrix} \tag{32}$$

In Fig. 5 the swashplate position behavior from the detailed simulation equation is compared with that from the simplified simulation using the steady state pressure assumption. An initial offset in the swashplate vertical position has been simulated. The agreement between the two simulations is not perfect, but is felt to be adequate (note the time and displacement scales in Fig. 5) in light of the order of magnitude reduction in the cost of simplified simulation runs vs detailed simulation runs. All of the results reported henceforth were generated with the simplified simulation.

Simulation of the responses of the swashplate position to a 1-cm vertical position step command applied at $t=0.1$ s with no pitch link loads present indicated that all three loop closure options yielded results indistinguishable from one another. This reflects the primary importance of position command-following to the control of the swashplate in each case.

Figures 6 and 7 illustrate the disadvantages of the Bypass control option and also illustrate the comparability of the PN and MN options. Both plots are of the total hydraulic energy expended in driving the swashplate as represented by the quantity [cf. Eq. (9)] $J=\Delta p^T\Delta p$. Figure 6 is for the case of the step input just discussed. The Bypass option used considerably more energy than either of the other two options, as can be seen. Also, the Minimum Norm option has a slight advantage over the Pressure-Null option, as would be expected since J is exactly the cost function minimized by the Minimum Norm strategy. However, the difference between MN and PN performance is essentially negligible for this case.

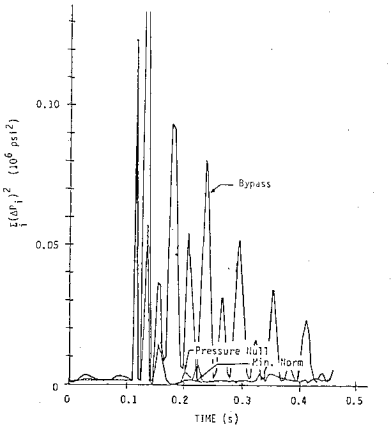

Fig. 6 Step response—no loads.

Figure 7 is for the extremely dynamic case of a 3500-lb load present on one of the pitch links with no other loads present. Thus, a large load rotates around the swashplate as the main rotor rotates. The results of all three control options are superimposed on the same plot. The MN option again enjoys a slight advantage over the PN option while the Bypass option produces erratic behavior in the energy expended due to its unfavorable geometry. The Bypass closure option is dropped from further consideration because of its clear inferiority.

Simulations were also run for a composite pitch link loading comprising 2750 lb at a spatial frequency of 5/revolution added to a 750-lb load at 8/revolution. This corresponds approximately to a stall/flutter loading pattern. The frequencies are not both multiples of four so as to ensure loading asymmetry. The results indicate that the Minimum Norm option performs slightly better than the Pressure Null option in terms of both the energy expended and the maximum loading. ("Maximum" here refers to the largest among the five actuators at each point in time.) Additionally, as Fig. 8 indicates, the maximum deviation of the differential pressure from the corresponding calculated Minimum Norm value is always a small percentage ($<10\%$) of the actuator loading. This relative size difference is crucial to the use of the pressure residuals for failure detection and identification purposes.

Finally, simulations involving opposing servovalve null offsets of ± 0.001 cm in two of the "active" actuators (as classified under the PN option) were run employing both the PN and MN options for control with no loads present. This case would ordinarily be expected to produce significant actuator force fighting. Figure 9 displays the results. The figure portrays the envelope containing the loading on the two actuators affected by the null offsets. Note the significant reduction in force fighting displayed by the Minimum Norm strategy.

The simulation was further modified to allow for random noise to be present in various quantities, to provide a mechanism for injecting failures into the system, and to encompass the simple actuator failure detection and identification (FDI) strategy described earlier. Here the results will briefly be described. Note that *all* of the results which follow are for the Minimum Norm loop closure option because only the Minimum Norm strategy maintains all five actuators equally active, thereby allowing for the application of direct comparison FDI techniques to the pressure residuals.

The modified simulation provides for white zero-mean Gaussian noise sequences of given intensity to be added to the following quantities: servovalve driving signal; source and drain pressure; actuator position measurements; actuator differential pressure measurements.

Also, the following failure modes can be introduced: P_2 becomes source pressure (hardover); P_2 becomes drain pressure (hardover); P_2 and P_1 both vanish (pressure loss, broken shaft); spool valve position freezes (at given position); bias (of given magnitude) in position sensor; bias (of given magnitude) in pressure sensor.

The FDI strategy incorporated into the simulation is of the simplest comparison type. Each actuator pressure residual is compared in magnitude to a specified threshold. If one or more of the residuals exceeds the threshold, the instrument associated with the largest residual magnitude is isolated as failed and its ram piston is bypassed. The remaining active loop closures are then reconfigured to implement a minimum norm strategy based on the four remaining operational actuators. No FDI is performed after one actuator has already been isolated because the remaining four actuators are then driving the three-degree-of-freedom swashplate dynamics, leaving a redundancy level of only one, thereby making possible only the detection and not the identification of a second failure by direct comparison techniques.

All of the results summarized here were generated by the steady-state pressure simulation with the stall/flutter load

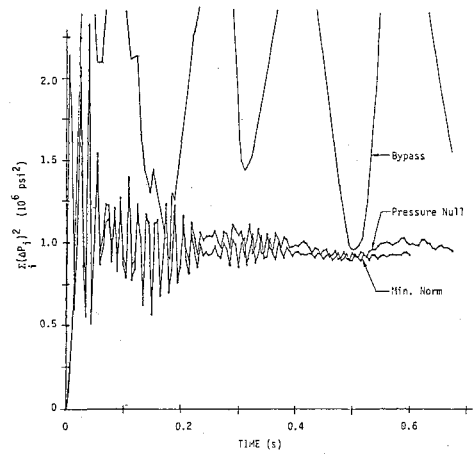

Fig. 7 Step response—3500 lb load on one actuator.

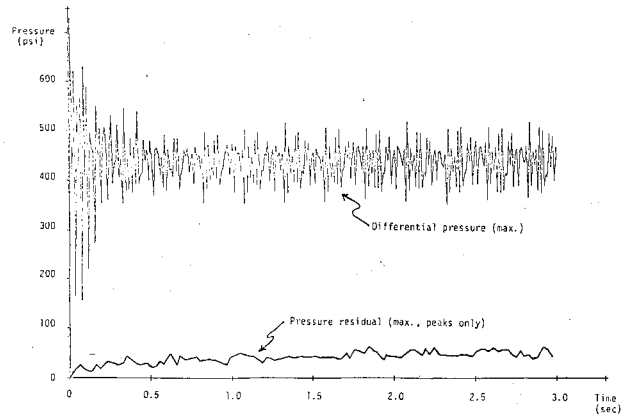

Fig. 8 Maximum differential pressure and peak values of maximum pressure residual for MN option.

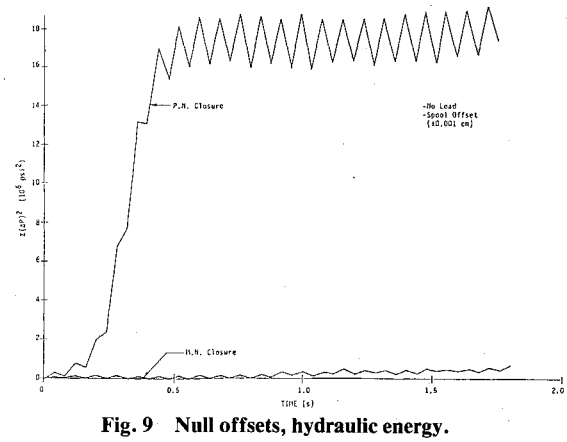

Fig. 9 Null offsets, hydraulic energy.

approximation discussed above. Furthermore, for all of the simulations the position sensor measurements were subject to additive noise with standard deviation $\sigma = 0.004$ cm (with one exception, which is noted) and the pressure sensors (again with one exception) had additive noise with $\sigma = 50\sqrt{2}$ psi. The threshold used was always 100 psi, which is approximately 1.4 σ. This threshold was chosen purely for testing purposes. A real system probably would utilize a larger threshold, which would avoid false alarms and also delay the detection of failures to some extent.

For a single case with the measurement noise intensities increased to $\sigma = 0.005$ cm for position and 141 psi for pressure

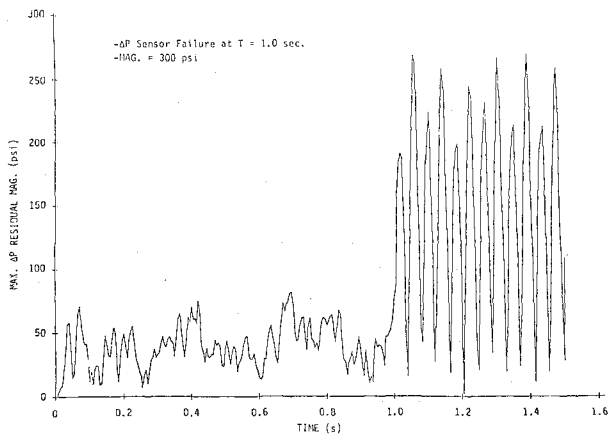

Fig. 10 Failure detection.

(the single exception to the values of 0.004 cm and $50\sqrt{2}$ psi mentioned above), a false alarm occurred at time = 0.63 s, at which time the minimum norm strategy for four actuators was implemented. The results indicated that the four pressure residuals after the false alarm exhibited symmetry. This reflects the loss of the degree of freedom in the residuals that is necessary for the isolation of a second failure. Hence, only a single failure is identifiable by algorithmic methods when five actuators are used.

A number of failure cases were simulated. The results for the case of a pressure sensor bias failure of 300 psi magnitude are illustrated in Fig. 10. The figure presents the maximum pressure residual as a function of time. The failure is inserted at time = 1.0 s and, as the figure shows, it is immediately detected. In fact, of the limited number of failure cases simulated, all exhibited immediate failure detection.

Summary and Conclusions

In this paper, two significant contributions to the area of helicopter swashplate control have been described, 1) The concept of minimum norm pressure feedback control for the purpose of reducing force-fights among redundant actuators via the minimization of expended hydraulic energy, and 2) the development of a dynamical simulation of the approximate swashplate dynamics when driven by multiple actuators.

The implementation of a minimum norm control strategy has been shown to be conducive to the use of decentralized local processing capability and also to accommodate the use of simple yet powerful comparison FDI tests. This appears to make it a strong candidate for any helicopter control system design where reliability and survivability are important considerations.

The simulation was used to compare the performance of the MN control strategy with two more conventional multiple actuator swashplate control strategies. The results indicate that the MN option always yields a performance that is at least comparable to, and can be significantly better than, the other options. In light of the other advantages of MN control, it would appear that MN may be the best control option for helicopter designs where energy consumption and reliability are of great concern.

Appendix: Derivation of Swashplate Simulation Equations

The basic approach to this development involves the assumption that the swashplate is a rigid body constrained to three degrees of motion freedom, one translational (collective) and two rotational (pitch and roll). This allows the writing of the one force and three moment equations for its motion with respect to the helicopter body. Decomposing the total inertial acceleration of the swashplate along the vertical body axis (or collective axis) which appears in the force equation into the components due to body motions, a gravity component, and the swashplate-body relative acceleration yields Eq. (14) directly after normalization by M_S'. The moment equations can be written with respect to helicopter axes and transformed to swashplate axes using Coriolis' Law. In swashplate-fixed coordinates, the rotational constraint $\omega_z = \dot{\omega}_z = 0$ yields two simultaneous differential equations for ω_x and ω_y, the solutions to which are Eqs. (15) and (16). The expressions for T_x and T_y are exceptionally complicated and are omitted for brevity. Equation (17) is the standard differential equation governing quaternion behavior where the rotational constraint has once again been applied.

The actuator shaft and pitch link shaft dynamics are derived in a fashion similar to the derivation of Eq. (14). That is, a force equation is written which governs the inertial acceleration of the actuator end and blade end of each shaft and the acceleration is decomposed into components including the relative acceleration of the two ends. After normalization by m_S'' or m_L'', the result is Eq. (18) or (19). Note that

$$f_{Ai} = -k_S \Delta s_i \qquad i = 1,\ldots,N \tag{A1}$$

and

$$f_{Lj} = -k_L \Delta \ell_j \qquad j = j,\ldots,N_L \tag{A2}$$

For each actuator, the pressure dynamics are given directly by Eq. (20). The quantities appearing therein include two quantities which can be expressed in terms of the swashplate and actuator shaft kinematics

$$\dot{z}_{Ri} = \dot{Z}_S - \dot{\Delta s}_i + r_A t_{33} (\omega_x y_i - \omega_y x_i) \tag{A3}$$

$$\Delta V = A_R \left[Z_S - \Delta s_i - r_A \frac{t_{31}}{t_{33}} x_i + \frac{t_{32}}{t_{33}} y_i \right] \tag{A4}$$

The flows Q_1 and Q_2 come from the standard orifice flow equations

$$Q_1 = C_w [A_{1S}(x_{S_i}) \sqrt{P_S - P_1} - A_{1D}(x_{S_i}) \sqrt{P_1 - P_D}] \tag{A5a}$$

$$Q_2 = C_w [A_{2S}(x_{S_i}) \sqrt{P_S - P_2} - A_{2D}(x_{S_i}) \sqrt{P_2 - P_D}] \tag{A5b}$$

Acknowledgments

The authors wish to thank J. Harrison of the Charles Stark Draper Laboratory for his contributions to this work. We also wish to acknowledge the support of Hamilton-Standard Division of United Technologies Corp. for the project upon which this work is based. Finally, we thank the reviewers for their comments which significantly enhanced the quantity of the paper.

References

[1] Carlock, G., Gatlin, C.M. Guinn, K.F., and Borgison, R.D., "STAR Flight Control System," *Proceedings of Flight Control Specialist Meeting of the American Helicopter Society,* Oct. 1978.

[2] Rapp, A., "Fly-by-Light Advanced Actuator System Characteristics for Dual (Active & On-Line) Operation Using Linear Drivers," Hamilton-Standard internal memo CD 907, Hamilton Standard Division, United Technologies Corp., Hartford, Conn., Oct. 1979.

[3] Brockett, R.W., *Finite Dimensional Linear Systems,* John Wiley & Sons, New York, 1970, pp. 126-127.

[4] Bryson, A.E., and Ho, Y.-C., *Applied Optimal Control,* rev. ed., Hemisphere (Wiley), New York, 1975, pp. 3-7.

[5] Daly, K.C., Gai, E., and Harrison, J.V., "Generalized Likelihood Test for FDI in Redundant Sensor Configurations," *Journal of Guidance and Control,* Vol. 2, Jan.-Feb. 1979, pp. 9-17.

[6] Kreysig, E., *Advanced Engineering Mathematics,* 3rd ed., John Wiley, New York, 1972, p. 641.

[7] Gai, E., Harrison, J., Walker, B., Weinstein, W., Desai, M., and Daly, K., "Advanced Flight Control System for Helicopters—Final Report," C.S. Draper Lab Rept. C-5381, Charles Stark Draper Laboratory, Cambridge, Mass., Dec. 1980.